


Dynamical response to supernova-induced gas removal in two-component spherical galaxies

Masahiro Nagashima¹  and Yuzuru Yoshii^{2,3}

¹*National Astronomical Observatory, Mitaka, Tokyo 181-8588, Japan*

²*Institute of Astronomy, School of Science, The University of Tokyo, Mitaka, Tokyo 181-0015, Japan*

³*Research Center for the Early Universe, School of Science, The University of Tokyo, Bunkyo-ku, Tokyo 113-0033, Japan*

13 November 2018

ABSTRACT

We investigate dynamical response on size and velocity dispersion to mass loss by supernovae in formation of two-component spherical galaxies composed of baryon and dark matter. Three-dimensional deprojected de Vaucouleurs-like and exponential-like profiles for baryon, embedded in truncated singular isothermal and homogeneous profiles for dark matter, are considered. As a more realistic case, we also consider a dark matter profile proposed by Navarro, Frenk & White. For simplicity we assume that dark matter distribution is not affected by mass loss and that the change of baryonic matter distribution is homologous. We found that the degree of the response depends on the fraction of dark matter in the region where baryon is distributed, so that dwarf spheroidal galaxies would be affected even in a dark halo if they are formed by galaxy mergers in the envelope of the dark halo. Our results suggest that this scenario, combined with dynamical response, would make not only the observed trends but the dispersed characteristics of dwarf spheroidals.

Key words: galaxies: dwarf – galaxies: elliptical and lenticular, cD – galaxies: evolution – galaxies: formation – galaxies: haloes – large-scale structure of the universe

1 INTRODUCTION

Elliptical galaxies have provided important information on the formation and evolution of galaxies. So far some scaling relations among photometric properties and global structural parameters have been observed, such as the colour–magnitude relation (e.g., Baum 1959), the velocity dispersion–magnitude relation (Faber & Jackson 1976), and the surface brightness–size relation (Kormendy 1977; Kodaira, Okamura & Watanabe 1983). These relations are regarded as clues to our understanding of galaxy formation.

It is widely believed that heating up and sweeping out the galactic gas by multiple supernova (SN) explosions play a key role on the formation of dwarf elliptical/spheroidal galaxies. In a traditional framework of monolithic cloud collapse scenario for formation of ellipticals, such multiple SNe cause a galactic wind to halt subsequent star formation and chemical enrichment (Larson 1969; Ikeuchi 1977; Saito 1979; Arimoto & Yoshii 1986, 1987; Kodama & Arimoto 1997). Since a large amount of gas is expelled by the galactic wind, the self-gravitating system expands after blowing up the wind (e.g., Hills 1980; Mathieu 1983; Vader 1986). Yoshii & Arimoto (1987) found that many observed properties of ellipticals can be reproduced by the galactic wind model with the evolutionary population synthesis technique. They noticed that theoretical metallicity of galaxies, to be compared with observation, should be an average of metallicities of constituent stars weighted by their luminosities. On the other hand, Dekel & Silk (1986) considered a model in which galaxies are embedded in dominant dark haloes. They claimed that structural properties of luminous matter would not be affected by the gas removal if dark matter dominates the gravitational potential. Their model can also reproduce the observed relations, although they did not take into account the evolutionary population synthesis. Recently, Zhao (2002) argued the dynamical limit on occurrence of galactic wind given by the existence of sufficiently dense dark halo and the absence of intergalactic/escaping globular clusters, and concluded that only about 4 per cent of the total mass of the galaxy should be lost by the wind.

In contrast to the monolithic cloud collapse scenario, recent studies on the cosmological structure formation suggest the hierarchical clustering scenario based on a cold dark matter (CDM) model. In this scenario, the CDM dominates the Universe gravitationally and objects

* E-mail: masa@th.nao.ac.jp

or dark haloes continuously cluster and merge together, so that larger objects form via mergers of smaller objects. Thus, simple galactic wind models must be modified in order to be consistent with the cosmological structure formation. Based on the hierarchical clustering scenario, semi-analytic models (SAMs) of galaxy formation have been developed (e.g., Kauffmann, White & Guiderdoni 1993; Cole et al. 1994, 2000; Somerville & Primack 1999; Nagashima, Gouda & Sugiura 1999; Nagashima et al. 2001, 2002). These models well reproduce many statistical observables of galaxies such as luminosity function, colour distribution, and gas fraction. Kauffmann & Charlot (1998) and Nagashima & Gouda (2001) have shown that their SAMs taking into account metal enrichment can reproduce the observed colour–magnitude relation of elliptical galaxies in clusters of galaxies and that this relation reflects the mass-metallicity relation, as pointed out by using the galactic wind model (Kodama & Arimoto 1997). Thus, as a next step, it is valuable to investigate not only the photometric properties but structural properties such as size and velocity dispersion. Moreover, Okamoto & Nagashima (2001a,b) found that radial gradients of fractional number, colour, and star formation rate of ellipticals in clusters are also reproduced by using the SAM associated with an N -body simulation.

Because a large amount of mass loss might occur during the formation of ellipticals, in both scenarios of monolithic cloud collapse and hierarchical clustering, it is important to construct a formalism on the dynamical response in two-component galaxies consisting of baryon and dark matter. While self-consistent equilibrium models of such two-component elliptical galaxies have been analysed by Yoshii & Saio (1987) and Ciotti & Pellegrini (1992), we focus on the dynamical response of baryon within a dark matter halo. In this paper we consider simple models of two-component galaxies in which the baryon having either de Vaucouleurs or exponential profile is embedded in the dark matter having either isothermal or homogeneous profile. Moreover, we also consider the so-called NFW profile of dark matter that is recently suggested by N -body simulations (Navarro, Frenk & White 1997).

This paper is outlined as follows. In section 2, general formulation for the dynamical response on size and velocity dispersion to mass loss is presented. In section 3 the dynamical response for particular choices of density distributions mentioned above is investigated. Section 4 summarizes the results of this paper. The details of models and derivations are given in Appendices.

2 EQUATIONS OF DYNAMICAL RESPONSE IN TWO-COMPONENT GALAXIES

We assume that the velocity fields of gas, stars and dark matter are non-rotating, homogeneous and isotropic characterized by a single parameter of velocity dispersion σ , and that the density distribution of baryon changes homologously. For simplicity, it is also assumed that the density distribution of dark matter does not change during the mass loss. This assumption will be justified for global structural parameters of dark matter because the total mass of dark matter dominates over baryon by a factor of 10 or so. Although the following results will be slightly modified in a dense region of baryonic matter because of non-negligible dynamical response on the local dark matter distribution, the resulting change of baryonic matter should be intermediate between the baryon-dominated and dark matter-dominated cases. We will study the dynamical response in such limiting cases in section 2.2.

The response depends on the timescale of gas removal between two extreme cases of adiabatic (slow) and instantaneous (rapid) gas removal. When the timescale is longer than the dynamical timescale of the system, it changes adiabatically in quasi-equilibrium. In this case the total change is a sum of consecutive infinitesimal changes. On the other hand, when the timescale of gas removal is much shorter than the dynamical timescale, the system drastically changes and it is possible that our assumption of homologous change might be broken. Under realistic circumstances, as hydrodynamical simulations suggest, these timescales are almost similar (e.g., Mori, Yoshii, Tsujimoto & Nomoto 1997; Mori, Yoshii & Nomoto 1999; Mori, Ferrara & Madau 2002). Therefore, keeping in mind that the adiabatic gas removal is more consistent with the situation under our assumptions, we consider both adiabatic and instantaneous gas removal below.

2.1 Formulation

A kinetic energy T due to velocity dispersion and a gravitational potential energy W of baryonic component in a dark matter halo are written as

$$T = \frac{1}{2} p \rho_b r_b^3 \sigma^2, \quad (1)$$

$$W = -a \rho_b^2 r_b^5 - b \rho_b \rho_d r_b^3 r_d^2 f(z), \quad (2)$$

respectively, where p, a and b are constants dependent on density distribution, ρ_b and ρ_d are characteristic densities of baryon and dark matter, respectively, σ is velocity dispersion of baryon, r_b and r_d are characteristic radii of baryon and dark matter, respectively, z is a radius r_b normalized by r_d , $z \equiv r_b/r_d$, and $f(z)$ is a function dependent on density distribution. Note that variables related to dark matter, with subscript d , do not change during the mass loss. From the virial theorem, we obtain

$$p \sigma_i^2 = a \rho_i r_i^2 + b \rho_d r_d^2 f(z_i), \quad (3)$$

$$p \sigma_f^2 = a \rho_f r_f^2 + b \rho_d r_d^2 f(z_f), \quad (4)$$

where subscripts i and f stand for the initial and final states, that is, before and after the mass loss, respectively, for the baryonic component. Just after the mass loss, only the baryon density changes from ρ_i to ρ'_i without any changes of other variables. Then, conserving its energy and mass, the system virializes again quickly to the final state,

$$\frac{1}{2}p\rho'_i r_i^3 \sigma_i^2 - a\rho'_i r_i^{2.5} - b\rho'_i \rho_d r_i^3 r_d^2 f(z_i) = \frac{1}{2}p\rho_f r_f^3 \sigma_f^2 - a\rho_f^2 r_f^{2.5} - b\rho_f \rho_d r_f^3 r_d^2 f(z_f). \quad (5)$$

After the mass loss the total mass of baryon also conserves, then $\rho'_i r_i^3 = \rho_f r_f^3$. By using this relation, the above equation is transformed to

$$\frac{p}{2}(\sigma_f^2 - \sigma_i^2) - a\rho_f r_f^2 \left(1 - \frac{r_f}{r_i}\right) - b\rho_d r_d^2 [f(z_f) - f(z_i)] = 0. \quad (6)$$

Using the virial relation, σ_i and σ_f can be eliminated as

$$1 + \frac{\rho_f}{\rho_i} \left[\left(\frac{z_f}{z_i}\right)^2 - 2 \left(\frac{z_f}{z_i}\right)^3 \right] + \frac{b\rho_d}{a\rho_i z_i^2} [f(z_f) - f(z_i)] = 0. \quad (7)$$

When the gas removal occurs instantaneously, the density at the final state is given by the above equation,

$$\frac{y_f}{y_i} = \frac{1 + b[f(z_f) - f(z_i)]/ay_i z_i^2}{(z_f/z_i)^2 (2z_f/z_i - 1)}, \quad (8)$$

where $y_{i,f} = \rho_{i,f}/\rho_d$, respectively. On the other hand, when the gas removal is sufficiently slow, the total change is a sum of consecutive infinitesimal changes, for which $y_f = y_i + dy$ and $z_f = z_i + dz$. Thus, linearizing the above equation, we obtain

$$\frac{dy}{dz} = -4\frac{y}{z} + \frac{b}{az^2} \frac{df(z)}{dz}, \quad (9)$$

where subscript i is omitted for simplicity. This corresponds to the case of adiabatic change. The first term in the above equation is obtained for the self-gravitational potential of baryon. The second term gives the modification for baryon embedded in dark matter. Solving this differential equation, we obtain

$$y = \frac{C}{z^4} + q(z), \quad (10)$$

where

$$q(z) \equiv \frac{b}{az^4} \int_0^z t^2 \frac{df(t)}{dt} dt, \quad (11)$$

and C is an integration constant. Since C is an adiabatic constant, the value does not change during the mass loss. Thus we obtain the density at the final state,

$$\frac{y_f}{y_i} = \frac{C/z_f^4 + q(z_f)}{y_i} = \frac{1}{y_i} \left[(y_i - q(z_i)) \frac{z_i^4}{z_f^4} + q(z_f) \right], \quad (12)$$

and

$$C = z^4 [y - q(z)] = z_i^4 [y_i - q(z_i)]. \quad (13)$$

From equations (3) and (4), the velocity dispersion at the final state is obtained as

$$\frac{\sigma_f}{\sigma_i} = \left[\frac{y_f z_f^2 + b f(z_f)/a}{y_i z_i^2 + b f(z_i)/a} \right]^{1/2}. \quad (14)$$

In the next section, we derive the dependence of y on z by specifying the function $f(z)$ in each case of density distributions of baryon and dark matter. Before studying such specific cases, we see the limiting cases of no dark matter and negligible baryonic matter in the next subsection.

2.2 Limiting cases

First, we consider the case of self-gravitating system with no dark halo, that is, $\rho_d/\rho_i \rightarrow 0$. The final form is expected to be the same as the result in Yoshii & Arimoto (1987). For instantaneous gas removal, we obtain from equation (7),

$$\frac{r_f}{r_i} \rightarrow \frac{M_f/M_i}{2M_f/M_i - 1}, \quad (15)$$

where $M_f/M_i = \rho_f r_f^3/\rho_i r_i^3$. This is the well-known result that the system becomes unbound if a half of the mass is removed. On the other hand, for adiabatic gas removal, the second term in equation (9) vanishes and then

$$\frac{\rho_f}{\rho_i} \rightarrow \frac{r_i^4}{r_f^4}. \quad (16)$$

The velocity dispersion is also obtained from equation (14),

$$\frac{\sigma_f}{\sigma_i} \rightarrow \left[\frac{\rho_f r_f^2}{\rho_i r_i^2} \right]^{1/2} = \frac{r_i}{r_f}. \quad (17)$$

Next, we consider the opposite case, $\rho_i/\rho_d \rightarrow 0$. As pointed out by Dekel & Silk (1986), the size and velocity dispersion of galaxies do not change during the mass loss because the gravitational potential is dominated by dark matter. Since the third term in equation (7) overwhelms other terms, z does not change against the change of y . Thus the velocity dispersion also does not change as obtained by equation (14). This case corresponds to that of §III-c in Dekel & Silk (1986).

Therefore, we confirm that our formulation is applicable to the limiting cases of no dark matter and negligible baryonic matter.

3 DYNAMICAL RESPONSE ON SIZE AND VELOCITY DISPERSION IN SPECIFIC CASES

In this section, we consider some specific density distributions. As for the baryonic component, we adopt the following two distributions. One is the Jaffe model (Jaffe 1983) that approximates the de Vaucouleurs profile when projected,

$$\rho(r) = \frac{4\rho_b r_b^4}{r^2(r + r_b)^2}, \quad (18)$$

where ρ_b and r_b are the characteristic density and radius, respectively. Another is a model that approximates the exponential profile when projected,

$$\rho(r) = \rho_b \sqrt{\frac{r_b}{r}} \exp \left[-g_{\text{exp}} \left(\frac{r}{r_b} - 1 \right) \right]. \quad (19)$$

The details of comparisons of these approximate profiles with the de Vaucouleurs and exponential profiles are given in Appendix A. As for the dark matter halo, we consider the following two distributions for truncated isothermal and homogeneous spheres,

$$\rho(r) = \rho_d \frac{r_d^2}{r^2} \theta(r_d - r), \quad (\text{isothermal}) \quad (20)$$

$$\rho(r) = \rho_d \theta(r_d - r), \quad (\text{homogeneous}) \quad (21)$$

respectively, where ρ_d is a characteristic density of dark matter and $\theta(x)$ is the Heaviside step function. Finally we also consider the NFW profile (Navarro, Frenk & White 1997),

$$\rho(r) = \rho_d c^3 \left[\frac{cr}{r_d} \left(1 + \frac{cr}{r_d} \right)^2 \right]^{-1}, \quad (22)$$

where c is the concentration parameter. Although Fukushige & Makino (1997, 2001) and Moore et al. (1998) suggest a modified NFW profile with steeper slope in the inner core, $\rho \propto r^{-1.5}$, we consider only the original NFW profile.

In a hierarchical clustering scenario, the isothermal profile should be applied to mergers and starbursts occurring near the centre of dark halo. This situation is realized when the mergers with satellite galaxies are caused by the dynamical friction. On the other hand, when satellite-satellite mergers occur in the envelope of dark halo by random collisions, the homogeneous profile should be applied. Recent high resolution N -body simulations suggest that many subhaloes survive and are not disrupted (e.g., Okamoto & Habe 1999; Moore et al. 1999; Ghigna et al. 2000). If their internal structures are also maintained, the isothermal profile should be applied even in the case of mergers in the envelope of dark halo. Moreover, outer parts of individual subhaloes near the centre of their host halo would be stripped by the tidal force from the host halo, then the mass ratio of baryon to dark matter would be high. We also consider such a case below.

3.1 de Vaucouleurs-like distribution of baryon in an isothermal dark halo

In this subsection, we investigate the dynamical response to mass loss in the case of isothermal dark halo. As already mentioned, we adopt the Jaffe model which well reproduces the deprojected three-dimensional de Vaucouleurs profile. The corresponding mass profile for baryon is

$$M_b(r) = \frac{16\pi\rho_b r_b^3 r}{r + r_b}, \quad (23)$$

and for dark matter,

$$M_d(r) = 4\pi\rho_d r_d^3 \left[\frac{r}{r_d} - \left(\frac{r}{r_d} - 1 \right) \theta(r - r_d) \right]. \quad (24)$$

In the following, we use a parameter m that stands for the mass ratio of baryon to dark matter,

$$m \equiv \frac{M_b(r \rightarrow \infty)}{M_d(r \rightarrow \infty)}. \quad (25)$$

From the self- and interaction-potential energies of baryon, we obtain the coefficients a and b in equation (2) as follows,

$$a = 128\pi^2 G, \quad \text{and} \quad b = 64\pi^2 G, \quad (26)$$

and the function $f(z)$ is

$$f(z) = \frac{\ln(1+z)}{z} + \ln\left(1 + \frac{1}{z}\right). \quad (27)$$

Substituting these quantities into equation (11) for adiabatic gas removal and into equation (8) for instantaneous gas removal, we obtain the dynamical response on size to gas removal. Moreover, using equation (14), we also obtain the response on velocity dispersion. Because the corresponding equations and solutions are complicated, we summarize those in Appendix B.

We examine how the dynamical response depends on the ratio of initial mass of baryon relative to dark matter halo $m_i \equiv M_i/M_d$ and the ratio of initial radius of baryonic component relative to dark matter halo $z_i \equiv r_i/r_d$. In the following we consider two representative values of $m_i = 0.2$ and 0.05 , and $z_i = 0.2$ and 0.05 , respectively. In a standard cosmological model, the baryon fraction is about 0.1 , so $m_i \simeq 0.1$ is expected if gas cooling is sufficiently effective. Thus the two values of m_i correspond to two extreme cases in realistic situations. The size of disk galaxies is usually considered to be a radius at which the disks are supported by their rotation under an assumption that their specific angular momenta conserve while the gas shrinks due to the cooling. The initial value of the specific angular momentum before the cooling is given by the so-called dimensionless spin parameter λ , which distributes log-normally around 0.05 , derived by the tidal torque due to the large-scale density inhomogeneity in the Universe (White 1984; Catelan & Theuns 1996a,b; Nagashima & Gouda 1997). Because an effective radius of disk is $\simeq \lambda r_{\text{vir}}$ (Fall 1983) and the size of elliptical galaxies is not significantly different from the disk size, the values of $z_i = 0.05$ and 0.2 are realistic. If outer parts of individual subhaloes are tidally stripped by their host halo, even larger values might be realized.

In the left panels of Figure 1, we plot the responses on size (upper panel) and velocity dispersion (lower panel) for $m_i = 0.2$. The thick solid and dashed lines indicate the results of $z_i = 0.2$ and 0.05 , respectively, for adiabatic gas removal. In the latter case of $z_i = 0.05$, because the baryonic component is compact and gravitationally dominates in the central region, the changes of size and velocity dispersion are larger than in the former case of $z_i = 0.2$. In the right panels, we show the results of $m_i = 0.05$. The changes are smaller when compared to those for $m_i = 0.2$ because of the small mass of baryonic component. Note that the changes for $(m_i, z_i) = (0.2, 0.2)$ and $(0.05, 0.05)$ are very similar to each other. The reason is, as pointed out by Navarro, Eke & Frenk (1996), that the changes can be measured by the value of m_i/z_i . If m_i/z_i is sufficiently small as shown by the thick solid line in the right panels ($m_i/z_i = 0.25$), the changes are negligible because the mass of dark matter dominates over the baryonic component. In such a case the assumption of dominant halo by Dekel & Silk (1986) can be justified.

For reference, we show the results for instantaneous gas removal by thin lines. As well known, the changes are greater than those for adiabatic gas removal. This tendency holds even in the dark matter-dominated case. Note that our results for this case are obtained under the assumption of homologous change, which might not be justified because some masses become unbound and leave the system. Actually, by using N -body simulations, Navarro, Eke & Frenk (1996) showed that some particles initially in the central region of a dark halo become unbound when a part of mass is instantaneously removed.

3.2 Dependence on dark matter distribution

In this subsection, we examine how the dynamical response depends on the density distribution of dark matter component, while the density distribution of baryonic component is fixed to the Jaffe model.

First we consider that the dark matter distributes homogeneously. The mass of dark matter within radius r is

$$M_d(r) = \frac{4\pi}{3} \rho_d r_d^3 \left[\frac{r^3}{r_d^3} - \left(\frac{r^3}{r_d^3} - 1 \right) \theta(r - r_d) \right]. \quad (28)$$

Then the coefficient b is

$$b = \frac{64}{3} \pi^2 G, \quad (29)$$

and the function $f(z)$ is

$$f(z) = \frac{1-2z}{2} + \frac{\ln(1+z)}{z} + z^2 \ln\left(1 + \frac{1}{z}\right). \quad (30)$$

In the same manner as before, we obtain the dynamical response on size and velocity dispersion for this case.

Next we consider the NFW profile. The mass within radius r is

$$M_d(r) = 4\pi \rho_d r_d^3 \left[\ln\left(1 + \frac{cr}{r_d}\right) - \frac{cr/r_d}{1 + cr/r_d} \right]. \quad (31)$$

The coefficient b is

$$b = 64\pi^2 G, \quad (32)$$

and the function $f(z)$ is

$$f(z) = \frac{c \ln(cz)}{1 - cz} + \frac{1}{z} [\ln(1 - cz) \ln(cz) + \text{Li}_2(cz)], \quad (33)$$

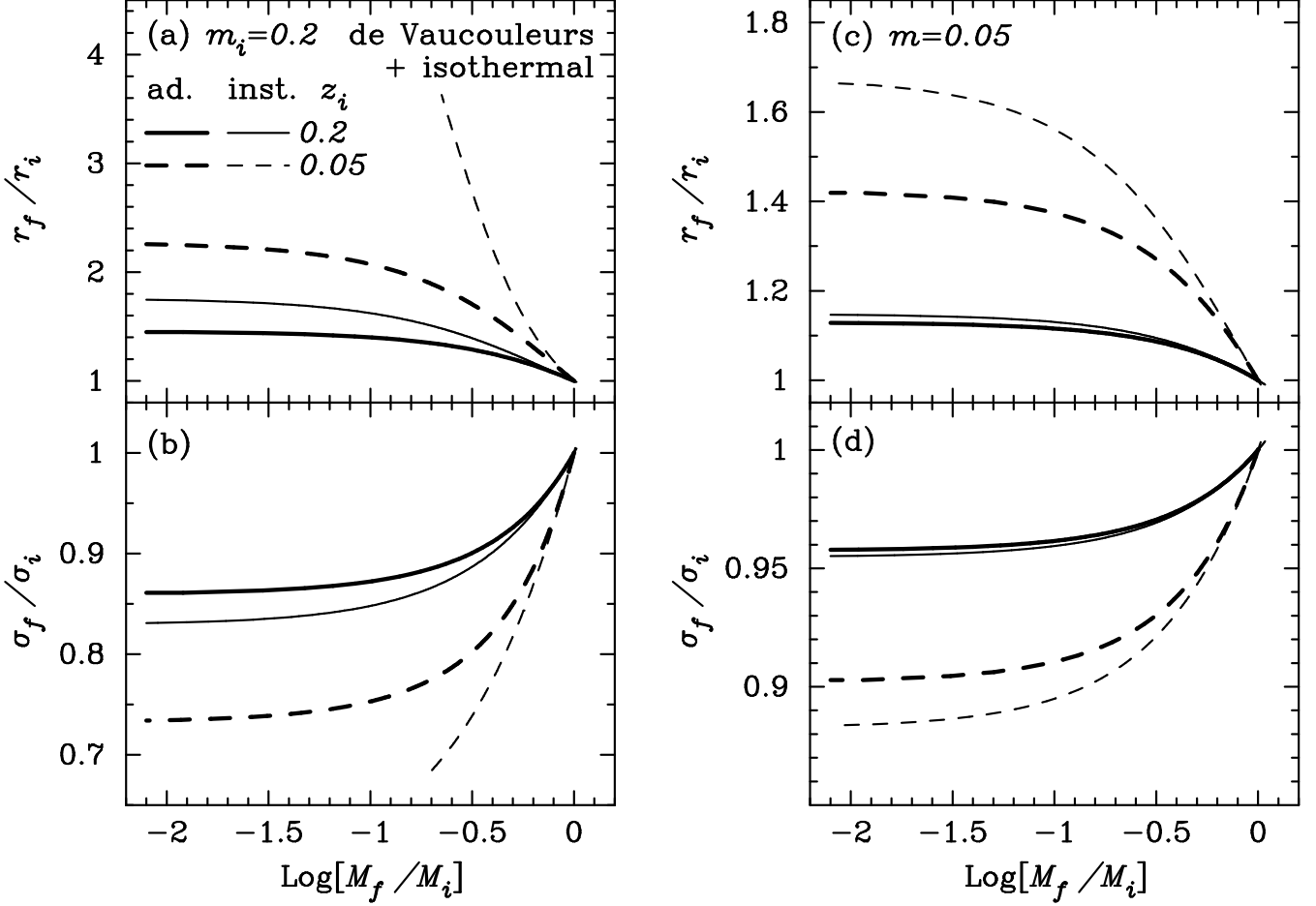


Figure 1. Dynamical response of the baryonic component of deprojected de Vaucouleurs profile embedded in an isothermal halo, for various values of initial mass $m_i \equiv M_i/M_d$ and size $z_i \equiv r_i/r_d$. The horizontal axis is the ratio of final to initial baryon masses. Upper and lower panels indicate the changes of size and velocity dispersion, respectively, for $m_i = 0.2$ (left panel) and 0.05 (right panel). The thick solid and thick dashed lines in each panel show the results of $z_i = 0.2$ and 0.05 , respectively, for adiabatic gas removal. The thin solid and thin dashed lines show those results for instantaneous gas removal. Note that the scales of vertical axes of left and right panels are different.

where $\text{Li}_2(z)$ is the dilogarithm. In defining the parameter m in equation (25), we truncate $M_d(r)$ at $r = r_d$, because it logarithmically diverges at $r \rightarrow \infty$. Otherwise we do not assume any truncation in the analysis.

The results for adiabatic gas removal are shown in Figure 2. The initial condition is $m_i = 0.2$ and $z_i = 0.05$ for all cases and $c = 10$ for the NFW profile. The solid, dashed and dot-dashed lines indicate the isothermal, homogeneous and NFW profiles, respectively. In the case of the homogeneous dark halo, we find that the changes of size and velocity dispersion are larger than those in the case of the isothermal halo and the influence from dark halo is weaker. This would reflect that the concentration of dark matter is lower than that of the isothermal halo and that the gravitational potential energy from dark matter is smaller, as indicated by the value of the coefficient b . This suggests that the size and velocity dispersion can be significantly affected by mass loss even if surrounded by dark matter, particularly when galaxy mergers frequently occur in the envelope of dark halo.

In the case of the NFW halo with $c = 10$, the responses are very similar to those for the isothermal halo. This is because these haloes have much the same density distributions.

3.3 Dependence on baryonic matter distribution

In this subsection, we examine how the dynamical response depends on the density distribution of baryon within a given halo. We consider the exponential-like distribution in the isothermal halo. The mass within r is

$$M_b(r) = \rho_b r_b^3 \frac{\pi e^g}{g^{5/2}} \left[-2 \sqrt{\frac{gr}{r_b}} \left(2 \frac{gr}{r_b} + 3 \right) \exp \left(-\frac{gr}{r_b} \right) + 3 \sqrt{\pi} \text{erf} \left(\sqrt{\frac{gr}{r_b}} \right) \right], \quad (34)$$

where we replace g_{exp} by g for simplicity. Then the coefficients a and b are

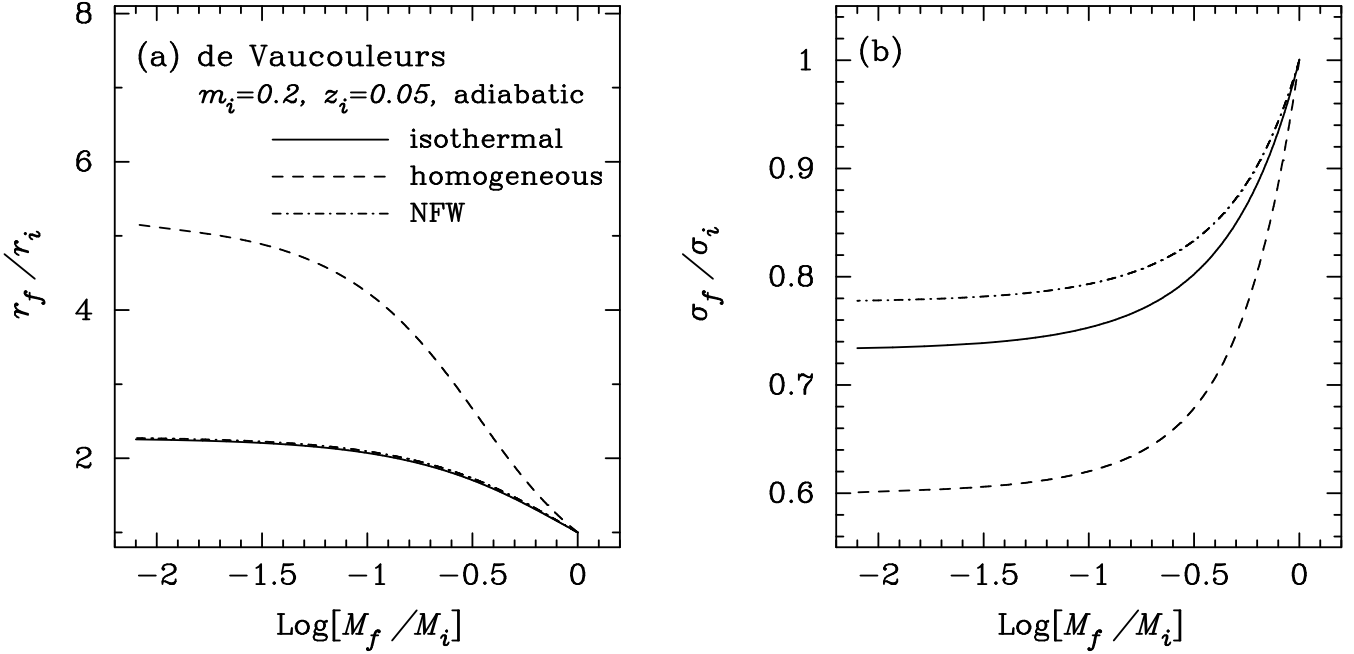


Figure 2. Dynamical response of the deprojected de Vaucouleurs component within a dark halo with three different profiles. The solid, dashed and dot-dashed lines denote the isothermal, homogeneous and NFW profiles, respectively. Shown are the responses on size (left panel) and velocity dispersion (right panel) only for adiabatic gas removal for the initial condition of $m_i = 0.2$ and $z_i = 0.05$.

$$a = \frac{\pi^2(3\pi - 4)e^{2g}}{g^4}G, \quad \text{and} \quad b = \frac{4\pi^2 e^g}{g^3}G, \quad (35)$$

and the function $f(z)$ is

$$f(z) = -\frac{2g \exp(-g/z)}{\sqrt{z}} + \sqrt{g\pi} \left\{ 3\gamma + \frac{2g}{z} - \left(5 + \frac{2g}{z} \right) \operatorname{erf} \left(\sqrt{\frac{g}{z}} \right) + \ln 64 + 3 \ln \left(\frac{g}{z} \right) \right\} + 3\sqrt{z} G_{23}^{30} \left(\frac{g}{z} \right)^{\left| \begin{smallmatrix} 3/2, 3/2 \\ 1/2, 1/2, 1 \end{smallmatrix} \right|}, \quad (36)$$

where γ is the Euler constant and G_{pq}^{mn} is the Meijer G function (this symbol should not be confused with the gravitational constant G).

The results for adiabatic gas removal are shown in Figure 3. Although we have calculated the exponential profile of baryonic component in the homogeneous halo (Appendix B4), we do not show this case in the figure, because the response is very similar to that for the de Vaucouleurs profile in the homogeneous halo. The dependence on the density distribution of baryonic component is weaker compared to that of dark matter component, which suggests that the response mainly depends on the density distribution of dark matter.

4 SUMMARY

We analyzed the dynamical response on structural parameters of elliptical galaxies to mass loss. While in the previous analyses only two limiting cases of pure self-gravitating baryonic system and dark matter-dominated system were considered (e.g., Yoshii & Arimoto 1987; Dekel & Silk 1986), we extended the formalism to the intermediate case between the two. Three-dimensional density distributions of baryonic matter considered in this paper are the Jaffe model that approximates the de Vaucouleurs profile and a model that approximates the exponential profile in two dimensions. As for the density distribution of dark matter, a truncated isothermal sphere and a homogeneous sphere are considered. As a more realistic case, we also considered the NFW dark matter halo which surrounds the baryonic component having de Vaucouleurs profile. Thus we found, from five combinations of baryon and dark matter, that the response strongly depends on the central concentration of dark matter, reflecting the fraction of baryon relative to dark matter in the central region. In contrast to the simple assumption by Dekel & Silk (1986) that structural parameters are not affected by mass loss, size and velocity dispersion can change even in dark matter, if baryon has sufficiently shrunk and become dense compared to dark matter at the onset of mass loss.

In this paper we considered both adiabatic and instantaneous gas removal. The adiabatic removal is justified if the timescale of gas removal is sufficiently slow compared to the dynamical timescale of the system. On the other hand, in the case of instantaneous gas removal, the effects of gas removal are stronger. For example, when more than a half of the mass is removed instantaneously, the pure self-gravitating system becomes unbound. Thus, our results for adiabatic removal place a lower limit on the dynamical response to mass loss. In order to check the opposite case, we also derived the results for instantaneous gas removal. As expected, the changes of size and velocity dispersion are larger than those for adiabatic gas removal. Such drastic changes may not validate our simple assumptions of homologous expansion of baryon and static distribution of dark matter.

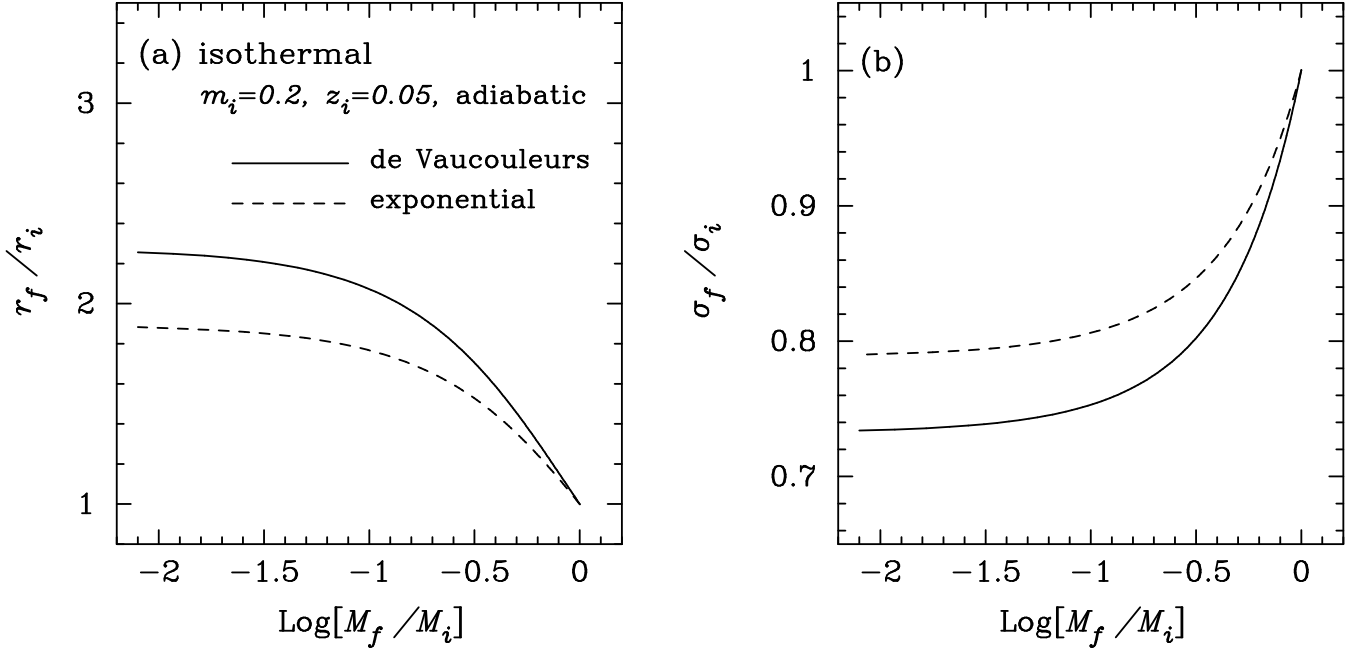


Figure 3. Dynamical response of the baryonic component within the isothermal dark halo. The solid and dashed lines denote the de Vaucouleurs and exponential profiles for the baryonic component, respectively. Shown are the responses on size (left panel) and velocity dispersion (right panel) only for adiabatic gas removal for the initial condition of $m_i = 0.2$ and $z_i = 0.05$.

So far some scaling relations such as the velocity dispersion-magnitude relation have been discussed considering the dynamical response to mass loss in the context of monolithic cloud collapse scenario for formation of elliptical galaxies. However, since the resulting structural change of baryonic component is found to depend significantly on the density distribution of dark matter, such scaling relations in the hierarchical clustering scenario should necessarily be reconsidered. Our results suggest that the dispersed properties of dwarf/compact ellipticals would be well reproduced by a variety of their formation histories and environment, when taking into account mass-dependent gas removal.

In the hierarchical clustering scenario, galaxy formation processes are rather complicated. There are many physical processes such as radiative gas cooling and galaxy merger as well as star formation and SN feedback. It should be noted that the physical mechanism of galaxy merger would be dynamical friction and/or random collision, while the mechanism of dark halo merger is growth of density fluctuation. In order to investigate the observed properties of galaxies, we need to fully incorporate the effects of dynamical response into realistic models of galaxy formation like our SAMs. We will discuss various observables of ellipticals in more realistic situations in a forthcoming paper.

ACKNOWLEDGMENTS

This work has been supported in part by the Grant-in-Aid for the Center-of-Excellence research (07CE2002) of the Ministry of Education, Culture, Sports, Science and Technology of Japan. Numerical computation in this work was partly carried out at the Astronomical Data Analysis Center of the National Astronomical Observatory and at the Yukawa Institute Computer Facility. The authors are grateful to the anonymous referee for helpful comments to improve the text and the figures.

REFERENCES

- Arimoto N., Yoshii Y., 1986, *A&A*, 164, 260
- Arimoto N., Yoshii Y., 1987, *A&A*, 173, 23
- Baum W.A., 1959, *PASP*, 71, 106
- Catelan P., Theuns T. 1996a, *MNRAS*, 282, 436
- Catelan P., Theuns T. 1996b, *MNRAS*, 282, 455
- Ciotti L., Pellegrini S., 1992, *MNRAS*, 255, 561
- Cole S., Aragon-Salamanca A., Frenk C. S., Navarro J. F., Zepf S. E., 1994, *MNRAS*, 271, 781
- Cole S., Lacey C. G., Baugh C. M., Frenk C. S., 2000, *MNRAS*, 319, 168
- Dekel A., Silk J., 1986, *ApJ*, 303, 39
- Faber S.M., Jackson R. E., 1976, *ApJ*, 204, 668

- Fall S. M., 1983, in ‘Internal kinematics and dynamics of galaxies’, proceedings of the IAU symposium 100, Besancon, France, Dordrecht, D. Reidel, p.391
- Fukushige T., Makino J., 1997, *ApJ*, 477, L9
- Fukushige T., Makino J., 2001, *ApJ*, 557, 533
- Ghigna S., Moore B., Governato F., Lake G., Quinn T., Stadel J., 2000, *ApJ*, 544, 616
- Gunn J.E., Gott J.R. 1972, *ApJ*, 176, 1
- Hills J.G., 1980, *ApJ*, 225, 986
- Ikeuchi S., 1977, *PTP*, 58, 1742
- Jaffe W., 1983, *MNRAS*, 202, 995
- Kauffmann G., White S. D. M., Guiderdoni B., 1993, *MNRAS*, 264, 201
- Kauffmann G., Charlot S., 1998, *MNRAS*, 294, 705
- Kodaira K., Okamura S., Watanabe M., 1983, *ApJL*, 274, L49
- Kodama T., Arimoto N., 1997, *A&A*, 320, 41
- Kormendy J., 1977, *ApJ*, 218, 333
- Larson R.B., 1969, *MNRAS*, 169, 229
- Mathieu R.D., 1983, 267, L97
- Moore B., Governato F., Quinn T., Stadel J., Lake G., 1998, *ApJL*, 499, L5
- Moore B., Ghigna S., Governato F., Lake G., Quinn T., Stadel J., Tozzi P., 1999, *ApJL*, 524, L19
- Mori M., Yoshii Y., Tsujimoto T., Nomoto K., 1997, *ApJL*, 478, L21
- Mori M., Yoshii Y., Nomoto K., 1999, *ApJ*, 511, 585
- Mori M., Ferrara A., Madau P., 2002, *ApJ*, 571, 40
- Nagashima M., Gouda N., 1997, *MNRAS*, 301, 849
- Nagashima M., Gouda N., Sugiura N., 1999, *MNRAS*, 305, 449
- Nagashima M., Gouda N., 2001, *MNRAS*, 325, L13
- Nagashima M., Totani T., Gouda N., Yoshii Y., 2001, *ApJ*, 557, 505
- Nagashima M., Yoshii Y., Totani T., Gouda N., 2002, *ApJ*, 578, 675
- Navarro J.F., Eke V.R., Frenk C.S., 1996, *MNRAS*, 283, L72
- Navarro J.F., Frenk C.S., White S.D.M., 1997, *ApJ*, 490, 493
- Okamoto T., Habe A., 1999, *ApJ*, 516, 591
- Okamoto T., Nagashima M., 2001a, *ApJ*, 547, 109
- Okamoto T., Nagashima M., 2001b, preprint, astro-ph/0108434
- Saito M., 1979b, *PASJ*, 31, 193
- Somerville R.S., Primack J. R., 1999, *MNRAS*, 310, 1087
- Vader J.P., 1986, *ApJ*, 305, 669
- White S.D.M., 1984, *ApJ*, 286, 38
- Yoshii Y., Arimoto N., 1987, *A&A*, 188, 13
- Yoshii Y., Saio H., 1987, *MNRAS*, 227, 677
- Zhao H., 2002, *MNRAS*, 336, 159

APPENDIX A: SIMPLE MODELS OF DENSITY DISTRIBUTION

A1 Approximate density distribution for the de Vaucouleurs $r^{1/4}$ profile

Most of elliptical galaxies have the so-called de Vaucouleurs $r^{1/4}$ luminosity profile,

$$\mu(R) = \mu_e \exp \left[-g_{\text{dV}} \left\{ \left(\frac{R}{R_e} \right)^{1/4} - 1 \right\} \right], \quad (\text{A1})$$

where $g_{\text{dV}} = 7.67$, R is the distance from the centre of luminosity distribution, and R_e is the effective half-light radius, at which the surface brightness reaches μ_e . In this paper, assuming that mass traces luminosity, we regard the surface brightness profile $\mu(R)$ as a surface mass density profile.

Since the de Vaucouleurs $r^{1/4}$ profile is two-dimensional projected density distribution, we need to reconstruct three-dimensional density distribution. A direct procedure is to use the Abel inversion between a surface density profile $\mu(R)$ and a three-dimensional density distribution $\rho(r)$,

$$\mu(R) = 2 \int_R^\infty \frac{\rho(r)r}{\sqrt{r^2 - R^2}} dr, \quad (\text{A2})$$

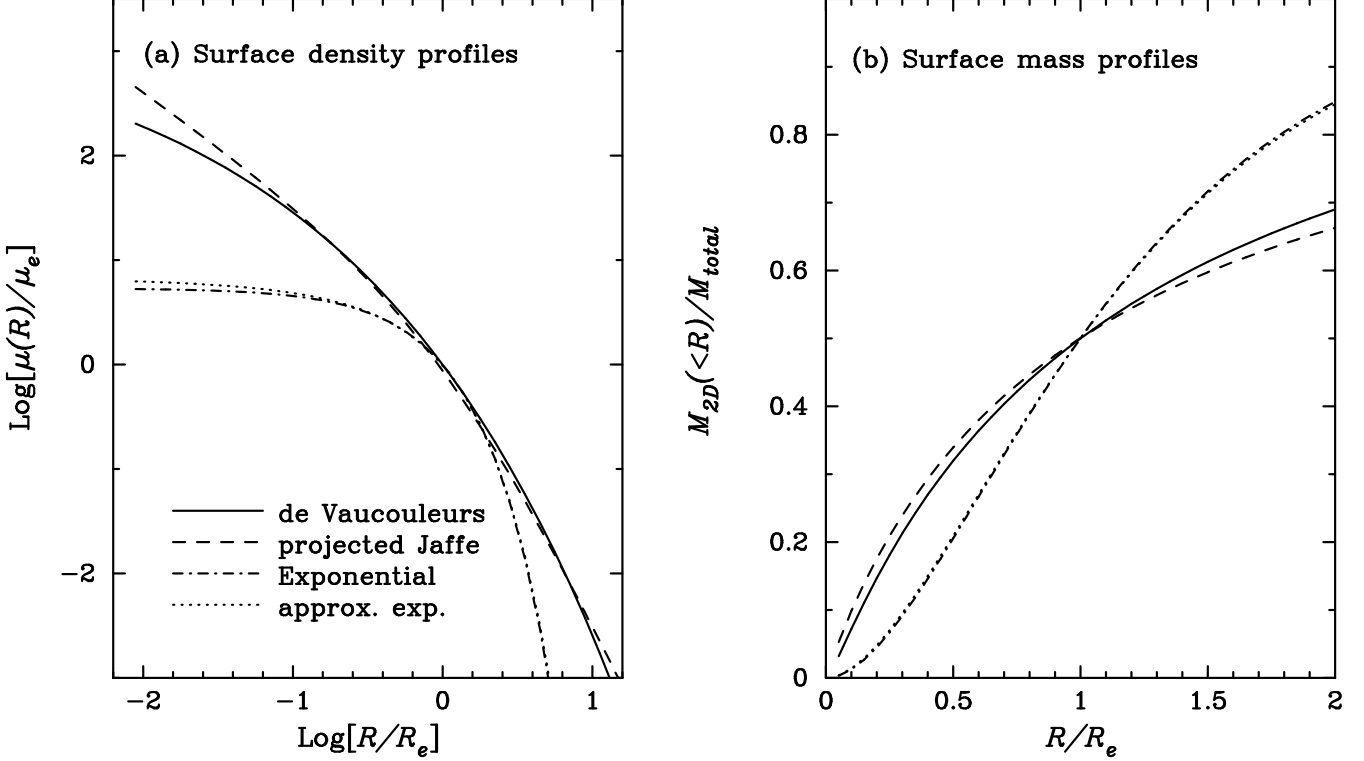


Figure A1. (a) Surface density plotted against R . This solid, dashed, dot-dashed, and dotted lines indicate the de Vaucouleurs profile, projected Jaffe model, exponential profile, and our approximated exponential model, respectively. (b) Surface mass within R . Lines are the same as in (a). Note that our approximated exponential model agrees fairly well with the exponential profile.

$$\rho(r) = -\frac{1}{\pi} \int_r^\infty \frac{d\mu(R)}{dR} \frac{dR}{\sqrt{R^2 - r^2}}. \quad (\text{A3})$$

However, since the obtained profile is generally not given by an analytic function, it is too complicated for analyses to use the exact profile. Therefore we adopt a simple, analytic model approximating the de Vaucouleurs profile when projected, that is, the Jaffe model (Jaffe 1983). By introducing characteristic density ρ_b and size r_b of baryonic matter, the density distribution $\rho(r)$ is written as follows,

$$\rho(r) = \frac{4\rho_b r_b^4}{r^2(r + r_b)^2}, \quad (\text{A4})$$

where the half-mass radius r_e in three-dimensional distribution coincides with r_b . The normalization of the density distribution is given by equating the total masses of the de Vaucouleurs and the Jaffe models. From this condition, we find

$$\rho_b = \frac{2520 \exp(g_{dV}) R_e^2}{g_{dV}^8 r_b^3} \mu_e. \quad (\text{A5})$$

Moreover, we also find that the relationship between three- and two-dimensional half-mass radii, r_e and R_e , is $R_e \simeq 0.744 r_e$. These relations lead to $\mu_e \simeq 4\rho_b r_e$.

The profile of surface density $\mu(R)$ and the profile of surface mass $M_{2D}(<R)$ within R are shown in Figure A1. The solid and dashed lines indicate the de Vaucouleurs profile and projected Jaffe model, respectively. We adopt the normalizations of density and size given by the above equations. As proved by many authors, the Jaffe model well reproduces the de Vaucouleurs profile.

A2 Approximate density distribution for the exponential profile

Spiral galaxies and dwarf elliptical galaxies have an exponential luminosity profile,

$$\mu(R) = \mu_e \exp \left[-g_{\text{exp}} \left(\frac{R}{R_e} - 1 \right) \right], \quad (\text{A6})$$

where $g_{\text{exp}} = 1.68$. Assuming the spherical symmetry, the deprojected three-dimensional density distribution using equation (A3) is expressed by the modified Bessel function of the second kind, $\mu_e g_{\text{exp}} \exp(g_{\text{exp}}) K_0(g_{\text{exp}} r/R_e) / \pi R_e$. However, because of simplicity, we use an approximate form for three-dimensional density distribution. Note that the modified Bessel function of the second kind K_0 is asymptotically proportional to $\exp(-g_{\text{exp}} r/R_e) / \sqrt{r}$ at $r \rightarrow \infty$. Then, to obtain a simple form expressed in elementary functions, we adopt the following density distribution

$$\rho(r) = \rho_b \sqrt{\frac{r_b}{r}} \exp \left[-g_{\text{exp}} \left(\frac{r}{r_b} - 1 \right) \right]. \quad (\text{A7})$$

As mentioned in the previous subsection, equating the total masses of these distributions, we find

$$\rho_b = \frac{2g_{\text{exp}}^{1/2} R_e^2}{3\pi^{1/2} r_b^3} \mu_e, \quad (\text{A8})$$

and $R_e \simeq 0.978r_b$. The half-mass radius r_e for three-dimensional distribution is given by $r_e \simeq 1.295r_b$, then $R_e \simeq 0.755r_e$. The projected density and mass profiles are also shown in Figure A1. The dot-dashed and dotted lines indicate the exponential profile and our approximated exponential model, respectively. It is found that the exponential profile is well reproduced by our model.

APPENDIX B: DERIVATIONS OF DYNAMICAL RESPONSE IN SPECIFIC CASES

In this section we derive the relation between density and size for the adiabatic change. [The instantaneous change can directly be solved by substituting the function $f(z)$ into equation (8).]

B1 de Vaucouleurs-like distribution of baryon in the isothermal dark halo

Using the density and mass distributions of baryon and dark matter, the self- and interaction-potential energies of baryon in the isothermal halo of dark matter are calculated by

$$-W_{\text{dV}}^{\text{self}} = 128\pi^2 G \rho_b^2 r_b^5, \quad (\text{B1})$$

$$-W_{\text{dV,iso}}^{\text{int}} = 64\pi^2 G \rho_b \rho_d r_b^3 r_d^2 \left[\frac{\ln(1+z)}{z} + \ln \left(1 + \frac{1}{z} \right) \right], \quad (\text{B2})$$

respectively. From equation (9), the differential equation for adiabatic gas removal is

$$\frac{dy}{dz} = -4\frac{y}{z} - \frac{\ln(1+z)}{2z^4}, \quad (\text{B3})$$

then we obtain a solution

$$y = \frac{C}{z^4} - \frac{1}{2z^4} [-z + (1+z) \ln(1+z)], \quad (\text{B4})$$

where C is an integration constant given by equation (13). In terms of mass instead of density, the response can be expressed by

$$m = 4yz^3, \quad (\text{B5})$$

where m denotes the mass ratio of baryon to dark matter.

B2 de Vaucouleurs-like distribution of baryon in the homogeneous dark halo

The interaction-potential energies of the de Vaucouleurs-like profile of baryon in the homogeneous halo of dark matter is

$$-W_{\text{dV,hom}}^{\text{int}} = \frac{64\pi^2}{3} G \rho_b \rho_d r_b^3 r_d^2 \left[\frac{1-2z}{2} + \frac{\ln(1+z)}{z} + z^2 \ln \left(1 + \frac{1}{z} \right) \right]. \quad (\text{B6})$$

The differential equation for adiabatic gas removal is

$$\frac{dy}{dz} = -4\frac{y}{z} - \frac{1}{6z^2} \left[2 - \frac{1}{z} + \frac{\ln(1+z)}{z^2} - 2z \ln \left(1 + \frac{1}{z} \right) \right]. \quad (\text{B7})$$

Then we obtain

$$y = \frac{C}{z^4} + \frac{1}{24z^4} \left[6z + z^2 - 2z^3 + 2z^4 \ln \left(1 + \frac{1}{z} \right) - 2(3+2z) \ln(1+z) \right], \quad (\text{B8})$$

where C is an integration constant. In terms of mass, we obtain

$$m = 12yz^3. \quad (\text{B9})$$

B3 Exponential-like distribution of baryon in the isothermal dark halo

The self-potential energy for baryon is given by

$$-W_{\text{exp}}^{\text{self}} = \frac{\pi^2 (3\pi - 4) e^{2g}}{g^4} G \rho_b^2 r_b^5, \quad (\text{B10})$$

and the interaction-potential energy for baryon embedded in the dark halo is

$$-W_{\text{exp,iso}}^{\text{int}} = G\rho_b\rho_d r_b^3 r_d^2 \frac{4\pi^2 e^g}{g^3} \times \left[-\frac{2g \exp(-g/z)}{\sqrt{z}} + \sqrt{g\pi} \left\{ 3\gamma + \frac{2g}{z} - \left(5 + \frac{2g}{z} \right) \text{erf} \left(\sqrt{\frac{g}{z}} \right) + \ln 64 + 3 \ln \left(\frac{g}{z} \right) \right\} + 3\sqrt{z} G_{23}^{30} \left(\frac{g}{z} \right)^{\left| \frac{3/2, 3/2}{1/2, 1/2} \right|} \right] \quad (\text{B11})$$

From this, the differential equation becomes

$$\frac{dy}{dz} = -4\frac{y}{z} + \frac{4g^3 e^{-g}}{(3\pi - 4)z^{9/2}} \left[-2\sqrt{\frac{\pi z}{g}} + 6\frac{z}{g} \exp\left(-\frac{g}{z}\right) + \sqrt{\pi} \left\{ 2\sqrt{\frac{z}{g}} - 3\left(\frac{z}{g}\right)^{3/2} \right\} \text{erf}\left(\sqrt{\frac{g}{z}}\right) \right], \quad (\text{B12})$$

then integrating the differential equation, we obtain

$$y = \frac{C}{z^4} + \frac{4g^{7/2} e^{-g}}{(3\pi - 4)z^4} \left[\exp\left(-\frac{g}{z}\right) \left\{ -2\sqrt{\frac{z}{g}} + 3\left(\frac{z}{g}\right)^{3/2} \right\} + 2\sqrt{\pi} \left\{ 1 - \frac{z}{g} - \left(1 - \frac{z}{g} + \frac{3}{4} \frac{z^2}{g^2} \right) \text{erf}\left(\sqrt{\frac{g}{z}}\right) \right\} \right], \quad (\text{B13})$$

where C is an integration constant. In terms of mass, we obtain

$$m = \frac{3\sqrt{\pi} e^g}{4g^{5/2}} y z^3. \quad (\text{B14})$$

B4 Exponential-like distribution of baryon in the homogeneous dark halo

The interaction-potential energy for baryon embedded in the dark halo is

$$-W_{\text{exp,hom}}^{\text{int}} = G\rho_b\rho_d r_b^3 r_d^2 \frac{\pi^2 e^g}{6g^{5/2}} \times \left[\frac{16g\sqrt{\pi}}{z} - 2 \exp\left(-\frac{g}{z}\right) \left\{ 8\sqrt{\frac{g}{z}} - 70\sqrt{\frac{z}{g}} - 105\left(\frac{z}{g}\right)^{3/2} \right\} - \sqrt{\pi} \left(105\frac{z^2}{g^2} - 36 + 16\frac{g}{z} \right) \text{erf}\left(\sqrt{\frac{g}{z}}\right) \right]. \quad (\text{B15})$$

Therefore the coefficient b is

$$b = \frac{\pi^2 e^g}{6g^{5/2}} G, \quad (\text{B16})$$

and the function $f(z)$ is

$$f(z) = \frac{16g\sqrt{\pi}}{z} - 2 \exp\left(-\frac{g}{z}\right) \left\{ 8\sqrt{\frac{g}{z}} - 70\sqrt{\frac{z}{g}} - 105\left(\frac{z}{g}\right)^{3/2} \right\} - \sqrt{\pi} \left(105\frac{z^2}{g^2} - 36 + 16\frac{g}{z} \right) \text{erf}\left(\sqrt{\frac{g}{z}}\right). \quad (\text{B17})$$

The differential equation for y is

$$\frac{dy}{dz} = -4\frac{y}{z} + \frac{g^{5/2} e^{-g}}{3(3\pi - 4)z^4} \left[\exp\left(-\frac{z}{g}\right) \left\{ 56 + 140\frac{z}{g} + 210\left(\frac{z}{g}\right)^2 \right\} - 8\sqrt{\pi} + \sqrt{\pi} \left\{ 8 - 105\left(\frac{z}{g}\right)^3 \right\} \text{erf}\left(\sqrt{\frac{g}{z}}\right) \right], \quad (\text{B18})$$

then integrating the differential equation, we obtain

$$y = \frac{C}{z^4} + \frac{g^{7/2} e^{-g}}{6(3\pi - 4)z^4} \times \left[\exp\left(-\frac{g}{z}\right) \sqrt{\frac{z}{g}} \left(-24 + 28\frac{z}{g} + 70\frac{z^2}{g^2} + 105\frac{z^3}{g^3} \right) + 8\sqrt{\pi} \left(3 - 2\frac{z}{g} \right) - \frac{\sqrt{\pi}}{2} \text{erf}\left(\sqrt{\frac{g}{z}}\right) \left(48 - 32\frac{z}{g} + 105\frac{z^4}{g^4} \right) \right], \quad (\text{B19})$$

where C is an integration constant. In terms of mass, we obtain

$$m = \frac{9\sqrt{\pi} e^g}{4g^{5/2}} y z^3. \quad (\text{B20})$$

B5 de Vaucouleurs-like distribution of baryon in the NFW dark halo

The NFW density distribution is written as

$$\rho(r) = \rho_d c^3 \left[\frac{cr}{r_d} \left(1 + \frac{cr}{r_d} \right)^2 \right]^{-1}, \quad (\text{B21})$$

where c is the concentration parameter. The mass within radius r is

$$M_d(r) = 4\pi\rho_d r_d^3 \left[\ln\left(1 + \frac{cr}{r_d}\right) - \frac{cr/r_d}{1 + cr/r_d} \right]. \quad (\text{B22})$$

The interaction-potential energy is

$$-W_{\text{dV,NFW}}^{\text{int}} = 64\pi G\rho_b\rho_d r_b^3 r_d^2 \left[\frac{c\ln(z)}{1-cz} + \frac{\ln(1-cz)\ln(cz) + \text{Li}_2(cz)}{z} \right], \quad (\text{B23})$$

where $\text{Li}_2(z)$ is the dilogarithm, $\int_z^0 [\ln(1-t)/t] dt$. The differential equation is

$$\frac{dy}{dz} = -4\frac{y}{z} + \frac{1}{2z^3} \left[\frac{c}{1-cz} - \frac{c(1-2cz)}{(1-cz)^2} \ln(cz) - \frac{\ln(1-cz)\ln(cz)}{z} - \frac{\text{Li}_2(cz)}{z} \right], \quad (\text{B24})$$

then integrating this equation, we obtain

$$y = \frac{C}{z^4} + \frac{1}{2cz^4} \left[-4cz + (4-cz)\ln(1-cz)\ln(cz) + \frac{cz(4-3cz)\ln(cz)}{1-cz} + (4-cz)\text{Li}_2(cz) \right], \quad (\text{B25})$$

where C is an integration constant. In terms of mass, we obtain

$$m = \frac{4yz^3}{\ln(1+c) - c/(1+c)}. \quad (\text{B26})$$

This paper has been typeset from a $\text{\TeX}/\text{\LaTeX}$ file prepared by the author.